

## FLUX PINNING IN MgB<sub>2</sub> THIN FILMS GROWN BY PULSED LASER DEPOSITION

M. Ionescu<sup>\*a</sup>, Y. Zhao<sup>a</sup>, M. Roussel<sup>a</sup>, S. X. Dou<sup>a</sup>, R. Ramer<sup>b</sup>, M. Tomsic<sup>c</sup>

<sup>a</sup>Institute for Superconducting & Electronic Materials, University of Wollongong, NSW 2522 Australia

<sup>b</sup>School of Electrical Engineering and Telecommunications, University of South Wales, Sydney 2052, Australia

<sup>c</sup>Hypertech Research Inc. OH, USA

A number of *c*-axis oriented MgB<sub>2</sub> thin films were grown *in-situ* by pulsed laser deposition (PLD) on Al<sub>2</sub>O<sub>3</sub>-R cut, and the pinning properties were investigated using transport, DC magnetisation and magneto-optical imaging (MOI) techniques. It was found that at temperatures below 10K and large applied DC magnetic fields, the irreversibility line of *in-situ* MgB<sub>2</sub> thin films is higher than a bulk material. The critical current density  $J_c$  of *in-situ* thin films is less dependent on the applied magnetic field  $B$  than the current density  $J_c$  of an *ex-situ* MgB<sub>2</sub> film or bulk. The penetration of magnetic field inside the film is uniform, and it follows the theoretical prediction for a homogenous thin film.

(Received October 14, 2003; accepted after revision January 30, 2004)

*Keywords:* MgB<sub>2</sub>, Thin films, Pulsed laser deposition, Superconductor, Flux pinning

### 1. Introduction

The discovery of superconductivity in MgB<sub>2</sub> with a transition temperature  $T_c = 39$  K [1], opens the possibility of replacing Nb<sub>3</sub>Sn ( $T_c = 18$  K) or Nb<sub>3</sub>Ge ( $T_c = 23$  K) used in superconducting magnets and electronic devices. In addition to a higher operating temperature, other advantages offered by this new superconductor are a simple structure, large coherence length ( $\xi \sim 5$  nm) [2] and large critical currents in high magnetic fields [3].

The MgB<sub>2</sub> material is known already for some time [4]. It has a hexagonal  $AB_2$ -type structure indexed in the space group  $P6/mmm$ , with B layers separated by Mg. Initially it was prepared in bulk form, and only recently in the form of wires, thin films and single crystals. For device applications, as well as for investigation of other superconducting properties, it is desirable to have epitaxial thin films. In particular high quality multi-layer epitaxial films are highly desirable for devices.

The main difficulties in growing high-quality MgB<sub>2</sub> films are the large difference in vapour pressure between magnesium and boron, and the high reactivity of magnesium with oxygen. For the PLD method, which is inherently a non-equilibrium process, the problem posed by the large difference in vapour pressure between magnesium and boron is difficult to overcome. The high reactivity of magnesium with oxygen can be overcome by reducing the amount of oxygen present in the deposition atmosphere.

In general, for MgB<sub>2</sub> thin films growth, two successful methods have been used so far. Encouraging results on various substrates were obtained for: a) a two-step procedure, which consists of B deposition followed by *ex-situ* Mg diffusion [5,6] and b) a single-step procedure, which consists of Mg and B deposition *in-situ* [7,8]. The best results reported so far in terms of  $T_c$  and  $J_c$  have been achieved using the two-step procedure.

---

\* Corresponding author: mionescu@uow.edu.au

So far all MgB<sub>2</sub> films grown by a single-step procedure were not epitaxial. Evidence of epitaxial growths was reported only for the two-step procedure, using RF sputtering of boron and post-deposition annealing in magnesium vapours at 850 °C [9]. However, from the devices point of view, the second fabrication method is more attractive for it is the only one capable to produce thin films with a multi-layer architecture. It is therefore desirable to improve the quality of MgB<sub>2</sub> films produced *in-situ*.

In this report we present results on the pinning properties of MgB<sub>2</sub> thin films grown *in-situ* by PLD, which include the effect of the deposition atmosphere and laser fluence on the stoichiometry of MgB<sub>2</sub> films.

## 2. Experimental

The MgB<sub>2</sub> thin films used in this work were produced using a standard PLD system. The PLD system comprises a UV excimer laser ( $\lambda = 248$  nm, pulse duration 25 ns); a fixed-beam optical train that focus the beam on a rotating target; a vacuum chamber with a base pressure of  $1 \times 10^{-7}$  Torr ( $7.5 \times 10^{-10}$  Pa).

The depositions of MgB<sub>2</sub> thin films were carried out on Al<sub>2</sub>O<sub>3</sub>-R, using two main routes. The first route (*in-situ*) started with a 5 min deposition from a stoichiometric MgB<sub>2</sub> target at a substrate temperature of 250 °C, and a 3 min deposition of a Mg cap layer from a Mg target, at the same temperature, at 130 mTorr (17.3 Pa) of high-purity Ar. This was followed by *in-situ* annealing at 680 °C for 10 min, at a pressure of 763 Torr of high-purity Ar. The MgB<sub>2</sub> film thickness obtained with this procedure was ~600 nm. The second route (*ex-situ*) started with a 10 min deposition from a B target, at a substrate temperature of 250 °C and 130 mTorr of high-purity Ar, followed by *ex-situ* annealing at 900 °C, in Mg vapours for 30 min. The MgB<sub>2</sub> film thickness obtained with this procedure was also ~600 nm. For all depositions, the optimum laser fluence was ~2.3 J/cm<sup>2</sup>, the repetition rate was 10 Hz, and the target-substrate distance was 25 mm.

As the Mg vapours are highly susceptible to oxidation, the level of oxygen in the chamber during the deposition process has to be strictly controlled. Possible sources of oxygen are the atmosphere of the chamber and the target. The first source can be greatly reduced by standard vacuum deposition procedures, such as low pressure, baking, flushing with dry gas, etc. The target may contribute to the level of oxygen in the deposition chamber mainly because of its porosity. It is particularly important to minimise this source of Mg oxidation since it is a very effective one. In our experiments we used a stoichiometric MgB<sub>2</sub> target having a density of 84% of the theoretical (X-ray) density, which was produced by hot isostatic pressing (HIP). An increase of target density above 84% was unsuccessfully attempted.

The optimisation of deposition conditions for the *in-situ* deposition route was carried out on three sets of films, produced at room temperature, at different laser fluences: ~1.3 J/cm<sup>2</sup>; ~1.8 J/cm<sup>2</sup>; and ~2.3 J/cm<sup>2</sup>. Each set contained five films, produced at different background pressures of high-purity Ar: 1 mTorr (0.133 Pa); 50 mTorr (6.65 Pa); 100 mTorr (13.3 Pa); 150 mTorr (19.95 Pa); and 200 mTorr (26.6 Pa).

The relative concentration of Mg and B of each film was measured by inductive coupled plasma spectroscopy (ICP), using a Varian Vista MPX axial spectrometer. The phase composition of targets and films was investigated by X-ray diffraction in  $\theta$ - $2\theta$  geometry, using a MAC Science three-independent axes diffractometer. Normal-to-superconducting transition temperatures  $T_c$  for the films were obtained by DC magnetization, on a SQUID magnetometer (Quantum Design MPMS system). The magnetic critical current density  $J_c$  was calculated using an extended Bean's model, from dc-magnetisation measurements up to an applied field of 5T, measured at different temperatures, using the same system mentioned above. Transport measurements were carried out using 4-probe technique at DC fields up to 9T, applied perpendicular to the (a,b) plane of the film. A Quantum Design PPMS system was used for this purpose. The local magnetisation behaviour of the optimally produced films was investigated by magneto-optic imaging (MOI), and compared with the theoretical predictions.

### 3. Results and discussion

In addition to the need for the chemical potential, the occurrence of the process of the stoichiometric condensation of MgB<sub>2</sub> films requires that both Mg and B have certain energy levels. For a fixed laser spot geometry, and target-substrate distance, these energy levels are controlled by laser fluence, and deposition pressure with opposite effects.

The variation of the relative concentration of Mg present on the substrate was measured by ICP, and presented in Fig. 1 as a function of laser fluence  $E$  and deposition pressure  $p$ . In this experiment we used three laser fluences ( $\sim 1.3$  J/cm<sup>2</sup>;  $\sim 1.8$  J/cm<sup>2</sup>;  $\sim 2.3$  J/cm<sup>2</sup>), and five deposition pressures (1 mTorr; 50 mTorr; 100 mTorr; 150 mTorr; 200 mTorr) of high purity Ar.

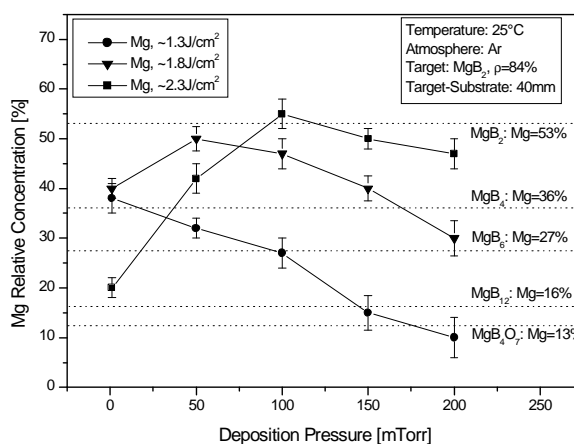


Fig. 1. Relative concentration of Mg on the substrate measured by ICP, and presented as a function of deposition pressure and laser fluence.

At the lowest fluence of  $\sim 1.3$  J/cm<sup>2</sup>, the relative concentration of Mg, measured on the substrate decreases continuously with the increase of the deposition pressure. On the same figure are represented the lines of constant Mg concentration in the main phases present in Mg-B-O system, which are close to MgB<sub>2</sub> in terms of Mg concentration.

The result shows that at the lowest fluence, the highest relative concentration of Mg measured on the substrate is  $\sim 40\%$  Mg. At this relative concentration, MgB<sub>2</sub> phase cannot be formed, since the stoichiometric MgB<sub>2</sub> contains 53% of Mg. In this case, other phases with a lesser Mg proportion are more likely to be formed, such as MgB<sub>4</sub>. At a higher laser fluence of  $\sim 1.8$  J/cm<sup>2</sup>, the relative concentration of Mg measured on the substrate is reaching a maximum of  $\sim 50\%$  Mg, at a deposition pressure of  $\sim 50$  mTorr.

This result shows that for lower deposition pressures, Mg has a too high energy in order to be retained on the substrate and form MgB<sub>2</sub>. On the other hand, for higher deposition pressures, the slowing down of Mg due to an increased number of collisions becomes predominant. As the result, the relative concentration of Mg on the substrate is decreasing, and again, the formation of MgB<sub>2</sub> film is less likely to take place.

At the highest fluence of  $\sim 2.3$  J/cm<sup>2</sup>, a similar dependence of the relative concentration of Mg versus the deposition pressure occurs. In this case however, the maximum is at  $\sim 55\%$  Mg, at a deposition pressure of  $\sim 100$  mTorr, and the relative concentration of Mg and B on the substrate allows the formation of MgB<sub>2</sub> film in-situ. These results are consistent with a recent spectroscopic investigation of the MgB<sub>2</sub> plasma dynamics in Ar atmosphere [10], which showed that for a background pressure higher than  $\sim 1.5$  mTorr, the time-of-flight distribution of Mg I emission line (383 nm), measured at a distance of 5 mm from the target, is continuous, indicating the onset of a slowing down effect of the Ar atmosphere.

These optimum conditions were used in the process of fabrication the MgB<sub>2</sub> films, as illustrated in Fig. 1, using a laser fluence of  $\sim 2.3$  J/cm<sup>2</sup> and a background pressure of high purity Ar,

of 130 mTorr. In addition, a repetition rate of 10 Hz and a deposition time of 10 min were used. After the deposition, a cap layer of pure Mg was deposited from a separate target, and the film was annealed *in-situ* at 680 °C for 10 min.

A second MgB<sub>2</sub> film was produced using an *ex-situ* procedure, which consisted of depositing a B film, approximately 600 nm thick, encapsulating the film in a pure Fe container, together with Mg powder, under an atmosphere of high purity Ar, and annealing the container at 900 °C for 30 min. The encapsulation was carried out as follows: the B film and the Mg powder were placed inside a Fe tube with one end closed; the procedure took place in a glovebox filled with high-purity Ar; the open end of the Fe tube was sealed with a valve, taken outside the glovebox; the Fe tube was sealed by pressing.

The X-ray orientation of the MgB<sub>2</sub> films is difficult to observe. Both, out-of-plane and in-plane signals are weak due to the small crystal size produced in the films. However, it can be said that the films are c-axis oriented. The in-plane orientation of the films should be attributed to the type of substrate used in this experiments. Indeed, Al<sub>2</sub>O<sub>3</sub> has a hexagonal structure (R-3cH), but the Al<sub>2</sub>O<sub>3</sub>-R cut substrate has a rectangular surface lattice, with the surface lattice constants  $a = 4.76 \text{ \AA}$  and  $b = 15.38 \text{ \AA}$ . A favourable (00l) orientation of the hexagonal MgB<sub>2</sub> film on such a surface could produce the following orientation relationship between the substrate and the film:  $[\bar{1}\bar{1}2] \text{ Al}_2\text{O}_3 \parallel [\bar{1}\bar{1}0] \text{ MgB}_2$ . This would result in a lattice mismatch of ~4% along  $[\bar{1}\bar{1}2] \text{ Al}_2\text{O}_3$  and ~35% along  $[\bar{1}\bar{1}0] \text{ Al}_2\text{O}_3$  directions. For such an orientation relationship, the film should have a 60° in-plane rotation relative to the substrate.

Previous research [11] suggested that the necessary conditions for epitaxial growth are a two-dimensional superlattice cell area of less than 60 nm<sup>2</sup>, and a lattice mismatch at the interface between the two-dimensional superlattice cells of less than 1%. These conditions had been verified experimentally on other film/substrate systems [12].

In the case of MgB<sub>2</sub>/Al<sub>2</sub>O<sub>3</sub>-R, the above conditions are not satisfied, and this could explain why the in-plane orientation of the film is poor. In the case of MgB<sub>2</sub>/(001)SiC the epitaxial growth condition mentioned above is satisfied [13]. So far there is only one report on MgB<sub>2</sub> film grown on SiC, but the transition temperature reported was low, at an onset of ~25 K, and the orientation of the film was not indicated [14].

The normal-to-superconducting transition temperature of the films produced *in-situ* was measured by the 4-probe method, in applied DC fields up to 9T, applied perpendicular to the substrate surface (parallel to the c-axis of the film). The results are presented in Fig. 2, and display weak field dependence. The inset of the figure shows the resistance versus temperature dependence in the range from room temperature to 5 K, at zero applied DC field. A residual resistance ratio (RRR) [ $\text{RRR} = R(300 \text{ K})/R(4 \text{ K})$ ] of 1.08 was obtained. This value is much smaller than the RRR for bulk MgB<sub>2</sub>, for which it can have values from 2 (our sample) to 20 [15], and even smaller than bulk MgB<sub>2</sub> doped with SiC, for which RRR is that of 1.74 [16]. This suggests that the pinning of the *in-situ* grown film is stronger than the bulk MgB<sub>2</sub>.

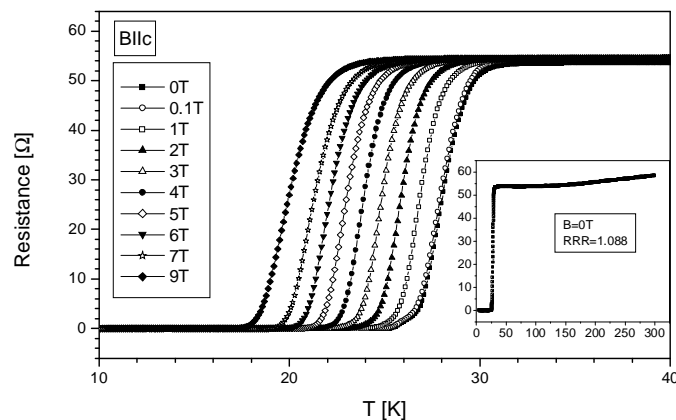


Fig. 2. Resistive transition in applied DC fields up to 9T for MgB<sub>2</sub> film grown *in-situ* by PLD. The inset shows the R-T curve at zero applied field for the same sample from 300 K down to 5 K.

The higher critical field  $H_{c2}^{\parallel}$  dependence on temperature, extracted from  $R(T, B)$  curves is presented in Fig. 3, together with the irreversibility line of bulk MgB<sub>2</sub> derived in the same way. It is evident that for temperatures below 20 K, the flux pinning for the in-situ film is stronger than in the bulk, in spite of the fact that the onset of superconducting transition in the film was 30 K, and in the bulk was 39 K.

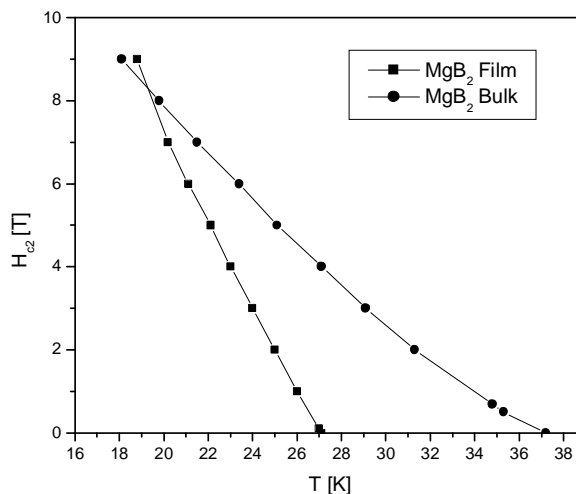


Fig. 3. Higher critical field ( $H_{c2}$ ) versus temperature for MgB<sub>2</sub> thin film grown *in-situ* by PLD, and for MgB<sub>2</sub> bulk.

The decrease in  $T_c$  between the bulk and thin film may be attributed to the influence, which a lower degree of crystallinity can have on the phonon spectrum of the MgB<sub>2</sub> crystal lattice [17].

The dynamics of magnetic flux penetration in MgB<sub>2</sub> film grown *in-situ* was investigated using MOI technique [18], using Fe-garnet as indicator film, deposited by magnetron sputtering. The DC probe field was 50 mT, applied parallel to the *c*-axis of the film, and the result at 20 K is presented in Fig. 4, where the bright square represent the location of the edges of the substrate.

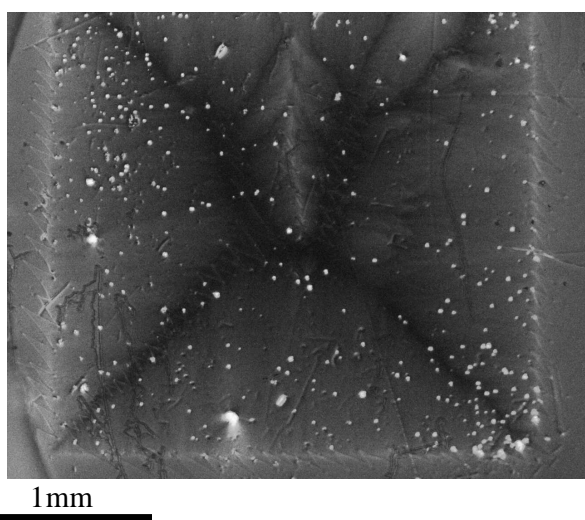


Fig. 4. MOI image of the magnetic flux penetration into a 3x3 mm<sup>2</sup> MgB<sub>2</sub> film, 600 nm thick, grown *in-situ* by PLD. The applied magnetic field of 50 mT was perpendicular to the (a, b) plane. The bright square contour is the edge of the film.

For the interpretation of the MOI we made use of numerical simulation of a perpendicular magnetic field  $B$  penetration into a rectangular film, characterised by  $B = \mu_0 H$ , and a highly non-linear I-V dependence, characteristic for HTS materials, at temperatures below  $T_c$ . This was based on one-dimensional integral equations for the sheet current, extended to describe time- and space-dependence [19,20,21]. The simulation was carried out in MATLAB environment, using Equation 1 [22,23]:

$$H_z(x, y) = H_a + \frac{J_c d}{4\pi} [f(x, y) + f(-x, y) + f(x, -y) + f(-x, -y)] \quad (1)$$

where:

$$f(x, y) = \sqrt{2} \ln \frac{\sqrt{2}P + a + b - x - y}{\sqrt{2}Q - a + b - x - y} + \ln \left| \frac{(P + y - b)(y - b + a)(P + x - a)}{(y - b)(Q + y - b + a)(x - a)(Q + x)} \right|$$

$$P = \sqrt{(a - x)^2 + (b - y)^2}$$

$$Q = \sqrt{x^2 + (b - a - y)^2}$$

And  $d$ , is the thickness, and  $a$  and  $b$  are the dimensions of the film.  $H_a$  represents the internal field from Ginzburg notation.

The simulation results are presented in Fig. 5. The sharp maxima of penetrated intensity of magnetic field  $H(x, y, t)$  at the edge of the film, and the sharp minima of  $H(x, y, t)$  at the current discontinuity lines represent the points where the self field of the supercurrents circulating in the film is zero, and therefore  $H(x, y, t)$  remains constant during the flux penetration, and equal to  $H_a$ . In the MOI image, these features are evidently similar with the simulation result, and this suggests that the film is homogenous.

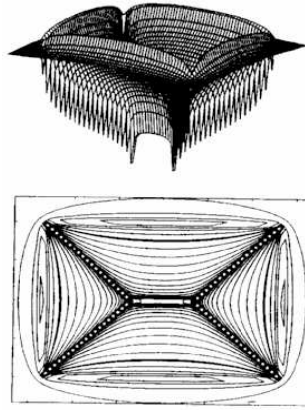


Fig. 5. Simulation of magnetic flux penetration into a thin film, applied perpendicular to (a,b) plane, using Equation 1.

The critical current density  $J_c$  versus magnetic field ( $B$ ), parallel with the  $c$ -axis, was calculated from the measurements of magnetic moment versus applied field ( $B$ ) for the films grown in-situ and ex-situ, using an extended Bean model, and the results are presented in Fig. 6. On the figure is also represented for comparison purposes the corresponding data for bulk  $MgB_2$ , obtained at 5 K. The values of  $J_c$  are presented here for comparative purposes. A reliable absolute value for magnetic  $J_c$  is difficult to obtain for thin films due to the highly inhomogenous field distribution, as shown above by numerical simulation.

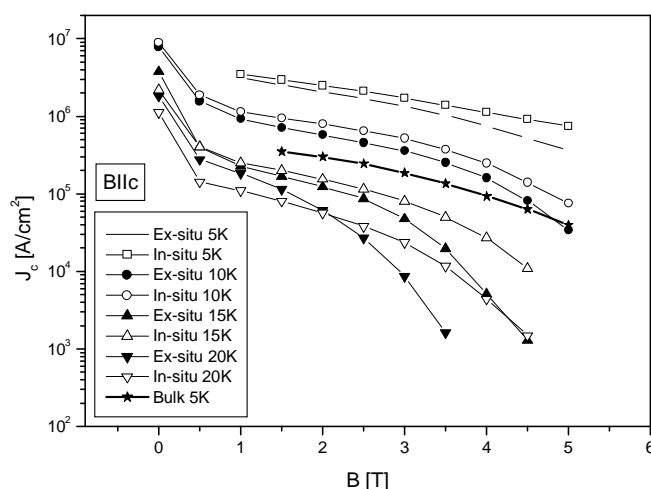


Fig. 6. Magnetic critical current density at different temperatures for MgB<sub>2</sub> film grown in-situ by PLD, and for MgB<sub>2</sub> film grown ex-situ, as described in text, as a function of applied magnetic field  $B$ , parallel to  $c$ -axis of the films.

Upon inspection of Fig. 6, we can see that the  $J_c$  of the *in-situ* grown films is higher at all measured temperatures than the *ex-situ* grown film, in spite of the higher transition temperature of the latter. This may be explained by the presence of a higher number of defects in the *in-situ* film as compared to the *ex-situ* film. Also, the field dependence of the *in-situ* film is better than for the *in-situ* film.

The  $J_c$  data at low temperature and low applied field is missing due to the strong magnetic flux instability (flux jump) under these conditions.

#### 4. Conclusions

It was shown that the optimised PLD deposition conditions for MgB<sub>2</sub> thin films led to in-situ deposited films with strong pinning. Below 10K and large DC magnetic fields, applied parallel to the  $c$ -axis of the film, the irreversibility line of in-situ MgB<sub>2</sub> thin films is higher than that of the bulk material. The critical current density  $J_c$  of in-situ thin films is less dependent on the applied magnetic field  $B$  than the current density  $J_c$  of an ex-situ MgB<sub>2</sub> film or bulk. In addition, it was shown by MOI that the in-situ films have homogenous pinning properties, a highly desirable feature for device applications.

#### Acknowledgement

The authors acknowledge the contribution of Dr E. H. Brandt for helpful discussions regarding the pinning in thin films and the simulation of field penetration.

#### References

- [1] J. Nagamatsu, N. Nakagawa, T. Muranaka, Y. Zenitani, J. Akimitsu, *Nature* **41**, 63 (2001).
- [2] C. B. Eom, M. K. Lee, J. H. Choi, L. Belenky, X. Song, L. D. Cooley, M. T. Naus, S. Patnaik, J. Jiang, M. Rikel, A. Polyanskii, A. Gurevich, X. Y. Cai, S. D. Bu, S. E. Babcock, E. E. Hellstrom, D. C. Larbalestier, N. Rogado, K. A. Regan, M. A. Hayward, T. He, J. S. Slusky, K. Inumaru, M. K. Haas, R. J. Cava, *Nature* **411**, 558 (2001).
- [3] W. N. Kang, H.-J. Kim, E.-M. Choi, C. U. Jung, S.-I. Lee, *Science* **292**(5521), 1521 (2001).

- 
- [4] X. H. Zeng, A. Sukiasyan, X. X. Xi, Y. F. Hu, R. Wertz, Q. Li, W. Tian, H. P. Sun, X. Q. Pan, J. Lettieri, D. G. Schlom, C. O. Brubaker, Z.-K. Liu, Q. Li, *Appl. Phys. Lett.* **79**(12), 1840 (2001).
- [5] A. Brinkman, D. Mijatovic, G. Rijnders, V. Leca, H. J. H. Smilde, I. Oomen, A. A. Golubov, F. Roesthuis, S. Harkema, H. Hilgenkamp, D. H. A. Blank, H. Rogalla *Physica C* **353**, 1 (2001).
- [6] C. B. Eom, M. K. Lee, J. H. Choi, L. J. Belenky, X. Song, L. D. Cooley, M. T. Naus, S. Patnaik, J. Jiang, M. Rikel, A. Polyanskii, A. Gurevich, X. Y. Cai, S. D. Bu, S. E. Babcock, E. E. Hellstrom, D. C. Larbalestier, N. Rogado, K. A. Regan, M. A. Hayward, T. He, J. S. Slusky, K. Inumaru, M. K. Haas, R. J. Cava *Nature* **411**, 558 (2001).
- [7] Y. H. Zhai, H. M. Christen, L. Zang, C. Cantoni, M. Paranthaman, B. C. Sales, D. K. Christen, D. H. Lowndes, *Appl. Phys. Lett.* **79**(16), 2603 (2001).
- [8] X. H. Zeng, A. Sukiasyan, X. X. Xi, Y. F. Hu, R. Wertz, Q. Li, W. Tian, H. P. Sun, X. Q. Pan, J. Lettieri, D. G. Schlom, C. O. Brubaker, Z.-K. Liu, Q. Li, *Appl. Phys. Lett.* **79**(12), 1840 (2001).
- [9] S. D. Bu, D. M. Kim, J. H. Choi, J. Gienke, S. Patnaik, L. Cooley, E. E. Hellstrom, D. C. Larbalestier, C. B. Eom, J. Lettieri, D. G. Schlom, W. Tian, X. Q. Pan, Preprint cond-mat/0204004.
- [10] S. Amoruso, R. Bruzzese, N. Spinelli, R. Velotta, X. Wang, C. Ferdeghini, Preprint cond-mat/0204374.
- [11] A. Zur, T. C. McGill, *J. Appl. Phys.* **55**, 378 (1984).
- [12] S. Shinkai, K. Sasaki, *Jpn. J. Appl. Phys.* **38**, 2097 (1999).
- [13] K. Ueda, M. Naito, *Appl. Phys. Lett.* **79**(13), 2046 (2001).
- [14] D. H. A. Blank, H. Hilgenkamp, A. Brinkman, D. Mijatovic, G. Rijnders, H. Rogalla, *Appl. Phys. Lett.* **79**(3), 394 (2001).
- [15] D. K. Finnemore, J. E. Ostenson, S. L. Bud'ko, G. Lapertot, P. C. Canfield, *Phys. Rev. Lett.* **86**, 2420 (2001).
- [16] S. X. Dou, S. Soltanian, J. Horvat, X. L. Wang, S. H. Zhou, M. Ionescu, H. K. Liu, P. Munroe, M. Tomsic, *Appl. Phys. Lett.* **81**, 3419 (2002).
- [17] C. Buzea, T. Yamashita, *Supercond. Sci. & Technol.* **14**, R115 (2001).
- [18] Ch. Joos, J. Albrecht, H. Kuhn, s. Leonhardt, H. Kronmüller, *Reports on progress in Physics* **65**, 651 (2002).
- [19] E. H. Brandt, *Phys. Rev. Lett.* **71**, 2821 (1993).
- [20] E. H. Brandt, *Phys. Rev. B* **49**, 9024 (1994).
- [21] E. H. Brandt, *Phys. Rev. B* **50**, 4034 (1994).
- [22] E. H. Brandt, *Phys. Rev. Lett.* **74**, 3025 (1995).
- [23] E. H. Brandt, *Phys. Rev. Lett.* **74**, 3499 (1995).